JOURNAL OF MOLECULAR SPECTROSCOPY **183,** 263–272 (1997)
ARTICLE NO. MS977295

Fourier Transform Emission Spectroscopy of ScH and ScD: The New Singlet Electronic States $A^1\Delta$, $D^1\Pi$, $E^1\Delta$, and $F^1\Sigma^-$

R. S. Ram* and P. F. Bernath*,†

*Department of Chemistry, University of Arizona, Tucson, Arizona 85721; and †Department of Chemistry, University of Waterloo, Waterloo, Ontario, Canada N2L 3G1

Received October 7, 1996; in revised form March 3, 1997

The emission spectra of ScH and ScD have been investigated in the near infrared and visible using a Fourier transform spectrometer. The molecules were excited in a scandium hollow cathode lamp operated with neon gas and a trace of hydrogen or deuterium. Apart from the $X^1\Sigma^+$, $B^1\Pi$, $C^1\Sigma^+$, and $G^1\Pi$ states reported previously [R. S. Ram and P. F. Bernath, *J. Chem. Phys.* **105,** 2668–2674 (1996)], four additional new singlet electronic states $A^1\Delta$, $D^1\Pi$, $E^1\Delta$, and $F^1\Sigma^-$ have been identified below 21 000 cm^{-1}. The rotational analysis of several vibrational bands of the $D^1\Pi$–$X^1\Sigma^+$, $D^1\Pi$–$A^1\Delta$, $E^1\Delta$–$B^1\Pi$, $E^1\Delta$–$A^1\Delta$, and $F^1\Sigma^-$–$B^1\Pi$ transitions has been carried out and spectroscopic constants have been determined. The $E^1\Delta$ state of ScH was not located because of the very weak intensity of the $E^1\Delta$–$B^1\Pi$ and $E^1\Delta$–$A^1\Delta$ transitions.

INTRODUCTION

In the past decade considerable progress has been made in understanding the electronic structure of transition metal hydrides, but until recently the electronic spectra of the IIIB transition metal hydride family (ScH, YH, LaH) were not well understood. For YH (*1–3*) and LaH (*4, 5*) new ab initio calculations and new spectroscopic analyses have been published. These recent studies are consistent with a $^1\Sigma^+$ ground state and a $^3\Delta$ state as the first triplet excited state.

Although the spectra of ScH and ScD have been known since 1973, the observed bands remained largely uncharacterized. Several visible bands of ScH and ScD were initially observed in absorption by Smith (*6*). This work was followed by the observation of emission bands of ScH and ScD in the visible and near infrared regions by Bernard *et al.* (*7*) who used a composite wall hollow cathode lamp. In addition to the bands previously observed by Smith (*6*), Bernard *et al.* (*7*) observed some additional bands at 789.74 and 860.35 nm for ScH and 859.6 nm for ScD. The bands had a complex appearance because of overlapping lines and perturbations. No rotational assignments of the ScH and ScD bands were made and the nature of the low-lying electronic states was uncertain.

Since ScH is the simplest transition-metal-containing molecule, there have been a large number of theoretical calculations of the spectroscopic properties of ScH (*8–13*). The CI calculations of Bauschlicher and Walsh (*8*), Anglada *et al.* (*9*) and Bruna *et al.* (*10*) all predict the ground state of ScH as a $^1\Sigma^+$ state with a close-lying $^3\Delta$ state. In addition Chong *et al.* (*12*) calculated the dipole moments for many hydrides of the 3*d* and 4*d* transition metals. In a recent paper Anglada *et al.* (*13*) reported the results of their extensive MRD-CI calculations on the electronic states of ScH related to the $3d^14s^2$, $3d^24s^1$, and $3d^14s^14p^1$ configurations of the Sc atom. They have predicted the spectroscopic properties of numerous excited electronic states as well as the transition dipole moments between many of the states.

Very recently we have reported on the analysis of several

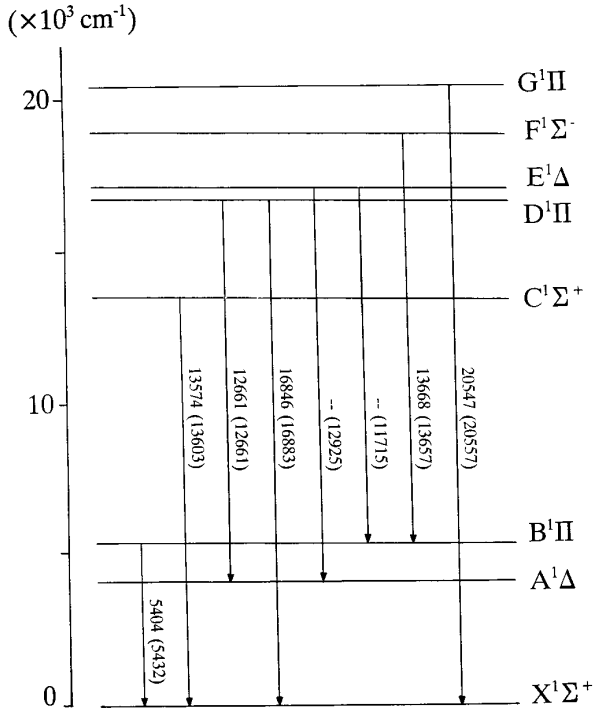

FIG. 1. A schematic energy level diagram of the observed singlet electronic states of ScH. The numbers marked with arrows are 0–0 origins of ScH and ScD (in brackets) of the observed transitions.

0022-2852/97 $25.00

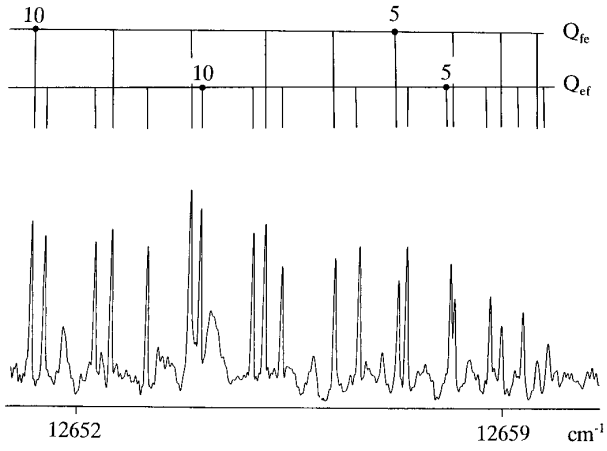

FIG. 2. An expanded portion of the spectrum of the 0–0 band of the $D^1\Pi$–$A^1\Delta$ system of ScH near the Q head. The perturbation observed at $Q_{ef}(8)$ can be seen clearly.

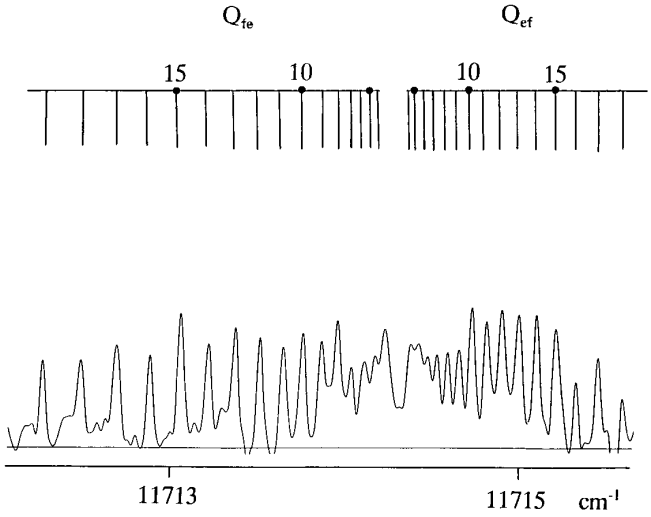

FIG. 4. An expanded portion of the spectrum of the 0–0 band of the $E^1\Delta$–$B^1\Pi$ system of ScD near the band origin.

bands of ScH and ScD in the 4000–21 000 cm^{-1} region (*14*). These bands were classified into three electronic transitions, $B^1\Pi$–$X^1\Sigma^+$, $C^1\Sigma^+$–$X^1\Sigma^+$, and $G^1\Pi$–$X^1\Sigma^+$, all having a common lower state. This state was assigned as the ground $X^1\Sigma^+$ state consistent with the ab initio predictions and the experimental results for the ScF, YH, and LaH molecules. As mentioned in the previous paper (*14*) many of the complex bands remained unclassified because of their weaker intensity, overlapping lines, and perturbations. In this paper we report on the rotational analysis of many of these bands and the identification of four more electronic states $A^1\Delta$, $D^1\Pi$, $E^1\Delta$, and $F^1\Sigma^-$. Nearly all of the low-lying singlet states of ScH and ScD are now known and the few remaining unassigned bands near 1 μm probably involve triplet states.

EXPERIMENTAL

The experimental details were provided in our previous paper (*14*). Briefly, the bands were excited in a scandium hollow cathode lamp and the spectra were recorded at 0.02 cm^{-1} resolution with the 1-m Fourier transform spectrometer associated with the McMath–Pierce Solar Telescope of the National Solar Observatory. The lamp was operated at 400 V with 570 mA current with a flow of 1.5 Torr Ne and about 40 mTorr of H_2 or D_2. The spectral line positions were extracted from the observed spectra using a data reduction program called PC-DECOMP developed by J. Brault. The peak positions were determined by fitting a Voigt lineshape function to each spectral feature.

In addition to the ScH and ScD bands, the spectra also contained many Sc and Ne atomic lines as well as ScN bands in the 5700–6500 cm^{-1} region which have been assigned previously to the $A^1\Sigma^+$–$X^1\Sigma^+$ transition (*15*). The measurements of the Ne atomic lines made by Palmer and Engleman (*16*) have been used for calibration of our ScH and ScD spectra. The absolute accuracy of the wave-

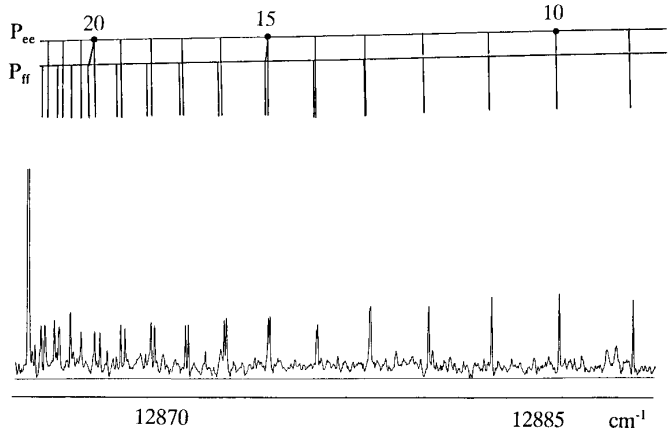

FIG. 3. An expanded portion of the P branch of the 0–0 band of the $E^1\Delta$–$A^1\Delta$ system of ScD.

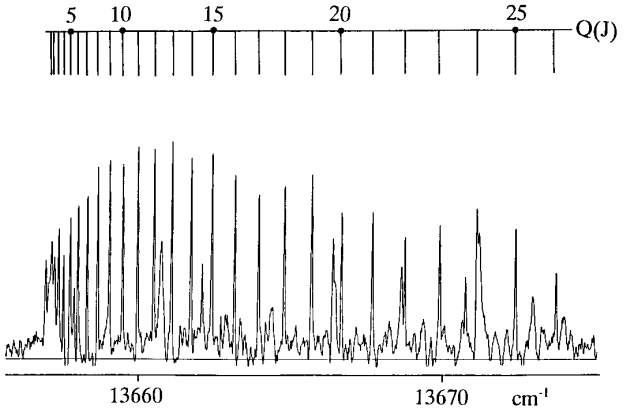

FIG. 5. An expanded portion of the spectrum of the 0–0 band of the $F^1\Sigma^-$–$B^1\Pi$ system of ScD near the Q head.

TABLE 1
Line Positions (in cm^{-1}) in the Observed Transitions of ScH

	$D^1\Pi - X^1\Sigma^+$ 0-0						$F^1\Sigma^- - B^1\Pi$ 0-0					
J	R(J)	O-C	P(J)	O-C	Q(J)	O-C	R(J)	O-C	P(J)	O-C	Q(J)	O-C
1											13667.378	-8
2	16868.534	1			16840.809	-0					13667.240	-7
3	16873.110	1			16836.025	-4	13706.556	0	13638.100	7	13667.039	-2
4	16876.154	-22	16793.547	4	16829.685	-4	13716.283	-2	13628.336	-0	13666.774	2
5	16877.762	6	16776.763	-3	16821.808	-7	13725.998	8	13618.615	4	13666.445	1
6	16877.887	16			16812.434	-4	13735.668	0	13608.925	-1	13666.065	3
7	16876.152	-393 *	16738.886	5	16801.597	4	13745.324	4	13599.296	2	13665.637	4
8	16873.804	-0	16717.860	18	16789.329	12	13754.945	-2	13589.729	1	13665.166	-1
9	16869.673	-1	16695.046	-406 *	16775.671	26 *	13764.549	-3	13580.240	-2	13664.673	-0
10	16864.177	-1	16671.734	-15	16760.658	42 *	13774.138	-5	13570.853	-1	13664.168	-2
11	16857.337	1	16646.768	-2	16744.521	258 *	13783.730	-1	13561.584	-1	13663.672	-3
12	16849.170	-1	16620.543	-6	16726.612	-7	13793.327	-3	13552.464	1	13663.217	-1
13	16839.690	-9	16593.122	3	16707.716	3	13802.962	-1	13543.520	1	13662.834	-1
14			16564.518	6	16687.577	6	13812.658	-1	13534.800	4	13662.577	4
15			16534.763	6	16666.214	-4	13822.460	1	13526.352	8	13662.505	2
16							13832.416	-3	13518.234	-1	13662.714	3
17							13842.603	-6			13663.314	-2
18							13853.127	4			13664.466	-4

	$D^1\Pi - A^1\Delta$ 0-0											
J	Ree(J)	O-C	Pee(J)	O-C	Rff(J)	O-C	Pff(J)	O-C	Qef(J)	O-C	Qfe(J)	O-C
2									12659.798	6	12659.618	4
3			12631.828	7			12631.648	4	12659.369	3	12659.012	-2
4	12704.722	-5	12622.096	3	12703.863	-7	12621.736	-5	12658.824	3	12658.234	-5
5	12713.250	-1	12612.262	1	12712.066	-8	12611.676	-6	12658.169	-1	12657.303	-7
6	12721.698	16	12602.340	-6	12720.148	3	12601.485	-7	12657.440	6	12656.246	-3
7	12729.629	-404 *	12592.375	4	12728.112	7	12591.198	-1	12656.648	17	12655.084	2
8			12582.360	2	12735.999	24 *	12580.834	4	12655.370	-412 *	12653.845	11
9	12746.549	-8	12571.912	-423 *	12743.815	42 *	12570.434	15	12654.888	-19	12652.551	23 *
10	12754.750	-1	12562.302	-20	12751.770	256 *	12560.019	27 *	12654.015	-6	12651.224	35 *
11	12762.925	15	12552.338	-5	12759.201	-12	12549.619	38 *	12653.142	-1	12650.094	258 *
12	12771.033	-3	12542.409	-5	12766.870	-5	12539.469	262 *	12652.280	-1	12648.478	-7
13	12779.134	2	12532.553	0	12774.500	-5	12528.893	-1	12651.446	0	12647.148	1
14	12787.198	-1	12522.779	7	12782.107	2	12518.656	-3			12645.832	1
15	12795.230	-5	12513.087	5	12789.680	5	12508.503	-10			12644.545	1
16	12803.251	1									12643.283	-3

Note: O-C are observed minus calculated values in the units of 10^{-3} cm^{-1} and asterisks mark perturbed lines (see text).

number scale is expected to be better than ± 0.002 cm^{-1}. The uncertainty of measurements of the weaker and blended lines are, however, expected to be somewhat larger depending on the signal-to-noise ratio, the extent of blending, and line broadening.

OBSERVATION AND ANALYSIS

The ScH bands located at 5404, 13 574, and 20 547 cm^{-1} have been assigned recently to the $B^1\Pi - X^1\Sigma^+$, $C^1\Sigma^+ - X^1\Sigma^+$, and $G^1\Pi - X^1\Sigma^+$ electronic transitions (*14*). The corresponding ScD bands have also been analyzed (*14*). The present paper deals with rotational analysis of the new transitions $D^1\Pi - X^1\Sigma^+$, $D^1\Pi - A^1\Delta$, and $F^1\Sigma^- - B^1\Pi$ of ScH and $D^1\Pi - X^1\Sigma^+$, $D^1\Pi - A^1\Delta$, $E^1\Delta - B^1\Pi$, $F'\Sigma^- - B'\Pi$, and $E^1\Delta - A^1\Delta$ transitions of ScD. In contrast to ScD, the bands involving the $E^1\Delta$ state of ScH were very weak in intensity and could not be rotationally analyzed. An energy level diagram of the singlet electronic states of ScH/ScD is provided in Fig. 1 and all of the marked states have been observed

TABLE 2
Line Positions (in cm^{-1}) in the Observed Transitions of ScD

$D^1\Pi - A^1\Delta$ 0-0

J	Ree(J)	O-C	Pee(J)	O-C	Rff(J)	O-C	Pff(J)	O-C	Qef(J)	O-C	Qfe(J)	O-C
3											12660.570	-16
4									12660.896	17	12660.718	6
5	12690.336	11							12661.126	6	12660.878	10
6	12695.480	-3	12632.216	6	12694.989	1			12661.412	-3	12661.057	1
7	12700.707	-2	12627.712	5	12700.041	1			12661.777	3	12661.274	-5
8	12706.028	1	12623.274	-0	12705.126	-1	12622.778	-1	12662.212	2		
9	12711.476	5	12618.925	-5	12710.264	4	12618.256	-4	12662.747	-1	12661.847	-0
10	12717.084	-1	12614.695	-3	12715.453	2	12613.799	-0	12663.424	3	12662.212	1
11			12610.617	2	12720.723	2	12609.409	3	12664.282	1	12662.646	2
12			12606.726	-3	12726.086	-8	12605.105	7			12663.168	-3
13					12731.609	4	12600.894	-3			12663.804	-11
14					12737.373	76 *	12596.826	-4			12664.610	-2
15					12743.530	307 *	12592.935	0			12665.688	81 *
16							12589.336	79 *			12667.158	304 *
17							12586.156	304 *				

$E^1\Delta - A^1\Delta$ 0-0 and $E^1\Delta - A^1\Delta$ 1-1

J	Ree(J)	O-C	Pee(J)	O-C	Rff(J)	O-C	Pff(J)	O-C	Ree+Rff	O-C	Pee+Pff	O-C
2									12904.912	18		
3	12945.774	1			12945.774	2			12910.462	0		
4	12951.637	-5	12906.357	12	12951.637	-4	12906.357	12	12916.231	1	12871.750	-4
5	12957.712	-0	12902.374	-5	12957.712	3	12902.374	-5	12922.191	-4	12867.868	1
6	12963.965	-14	12898.626	-3	12963.965	-8	12898.626	-1	12928.350	-2	12864.196	4
7	12970.434	-3	12895.093	-0	12970.434	6	12895.093	2	12934.698	2	12860.745	19
8	12977.074	-11	12891.768	-1	12977.074	3	12891.768	4	12941.229	6	12857.471	2
9	12983.903	-13	12888.654	-4	12983.903	8	12888.654	5	12947.942	16	12854.417	-1
10	12990.921	-4	12885.752	-5	12990.921	25	12885.752	9	12954.796	-3	12851.565	-4
11	12998.084	-25	12883.050	-11	12998.084	16	12883.050	8			12848.914	-4
12	13005.455	-4	12880.557	-14	13005.403	-1	12880.557	14			12846.468	4
13	13012.973	3	12878.284	1	13012.897	-0	12878.243	-1				
14	13020.632	-5	12876.193	1	13020.540	-2	12876.141	1				
15	13028.456	4	12874.298	2	13028.334	3	12874.225	-2				
16	13036.449	41	12872.593	2	13036.267	10	12872.499	-3				
17			12871.068	-3	13044.327	14	12870.956	-3				
18			12869.734	0			12869.596	1				
19			12868.575	2			12868.403	2				
20			12867.584	-1			12867.375	-2				

$E^1\Delta - B^1\Pi$ 0-0

J	Ree(J)	O-C	Pee(J)	O-C	Rff(J)	O-C	Pff(J)	O-C	Qef(J)	O-C	Qfe(J)	O-C
3	11734.397	6			11734.501	5						
4	11739.371	-0			11739.554	7			11714.363	-26	11714.216	4
5	11744.333	-1			11744.592	-3			11714.413	-13	11714.156	-3
6	11749.273	-3			11749.640	-0			11714.466	-4	11714.093	-4
7	11754.200	3	11678.842	-10	11754.682	1	11679.347	4	11714.520	-2	11714.020	-3
8	11759.094	-0			11759.717	3	11674.405	-3	11714.582	0	11713.936	-2
9	11763.969	1	11668.702	-8	11764.740	2	11669.502	9	11714.649	1	11713.842	-2
10	11768.821	4			11769.752	-0	11664.601	3	11714.724	0	11713.734	-2
11	11773.637	0	11658.592	2	11774.758	6	11659.724	-2	11714.809	3	11713.619	1
12	11778.428	-1	11653.537	-4	11779.736	-2	11654.871	-7	11714.899	3	11713.485	-2
13	11783.194	2	11648.516	12	11784.704	-2	11650.047	-6	11714.997	2	11713.345	-1
14	11787.929	5	11643.482	3	11789.656	-1	11645.254	-1	11715.104	3	11713.187	-4
15	11792.623	0	11638.470	2	11794.583	-3	11640.473	-10	11715.216	1	11713.021	-2
16	11797.286	-3	11633.473	2	11799.490	-3	11635.710	-27	11715.335	-2	11712.843	1
17	11801.915	-6			11804.379	5			11715.465	-2	11712.647	0
18					11809.228	-1			11715.607	0	11712.440	2
19									11715.737	-16	11712.215	1

TABLE 2—*Continued*

	$F^1\Sigma^+ - B^1\Pi$ 0-0						$F^1\Sigma^+ - B^1\Pi$ 1-1					
J	R(J)	O-C	P(J)	O-C	Q(J)	O-C	R(J)	O-C	P(J)	O-C	Q(J)	O-C
2									13703.223	-22	13713.217	0
3	13677.815	9	13642.192	1	13657.354	2			13698.402	-4	13713.337	-3
4	13683.120	-1	13637.344	-6	13657.518	-3			13693.625	-2	13713.510	2
5	13688.489	0	13632.574	-1	13657.731	-3	13743.885	-2	13688.908	-3	13713.829	108
6	13693.909	0	13627.868	-2	13657.988	-3	13749.206	14			13713.995	13
7	13699.380	1	13623.234	-3	13658.290	-1	13754.550	4	13679.683	6	13714.297	8
8	13704.903	3	13618.673	-3	13658.637	-0	13759.948	0	13675.169	2	13714.647	3
9	13710.474	5	13614.194	3	13659.028	-1	13765.393	-4	13670.732	2	13715.045	1
10	13716.091	4	13609.787	3	13659.468	1	13770.888	-5	13666.372	4	13715.481	-3
11	13721.755	3	13605.462	5	13659.955	1	13776.420	-13	13662.079	-4	13715.960	2
12	13727.466	1	13601.217	4	13660.491	3	13781.974	-42	13657.872	-6	13716.461	4
13	13733.225	1	13597.054	0	13661.074	1	13787.655	15	13653.740	-13	13716.923	-42 *
14	13739.024	-4	13592.983	2	13661.709	1	13793.300	-3	13649.675	-33	13717.264	-201 *
15	13744.883	4	13589.001	1	13662.390	-5	13798.990	-13	13645.765	19		
16	13750.772	-2	13585.102	-7	13663.139	4	13804.742	5	13641.881	13	13719.307	964 *
17	13756.712	-2	13581.317	4	13663.929	1	13810.511	3	13638.079	1	13719.852	1194 *
18	13762.690	-9	13577.614	-1	13664.778	-0	13816.314	-4	13634.384	0	13720.613	1769 *
19	13768.731	4	13574.012	-3	13665.679	-5					13721.488	2632 *
20	13774.797	-4	13570.508	-9	13666.654	7					13722.439	3793 *
21	13780.912	-6	13567.124	1	13667.670	1					13723.474	5311 *
22	13787.078	-1	13563.833	-3	13668.749	-2					13724.565	7213 *
23	13793.300	16	13560.660	4	13669.892	-3					13725.739	9581 *
24	13799.535	2	13557.590	1	13671.100	-2					13726.973	12448 *
25	13805.827	-0	13554.632	-3	13672.370	-2					13728.277	15878 *
26	13812.170	2	13551.797	-1	13673.710	1						
27	13818.556	2	13549.087	5	13675.114	0						
28	13824.993	6	13546.490	4	13676.591	3						
29	13831.478	9	13544.016	-1	13678.135	1						
30	13837.995	-7	13541.688	11	13679.757	2						
31			13539.462	-9	13681.453	-1						

TABLE 2—*Continued*

	$F^1\Sigma^+ - B^1\Pi$ 2-2						$D^1\Pi - X^1\Sigma^+$ 0-0	
J	R(J)	O-C	P(J)	O-C	Q(J)	O-C	Q(J)	O-C
3					13768.134	-3	16878.666	-6
4			13748.764	-4	13768.313	2	16875.991	4
5			13744.152	7	13768.529	-1	16872.633	1
6	13803.388	5	13739.591	5	13768.795	-1	16868.611	-0
7	13808.649	-3	13735.101	3	13769.107	-1	16863.920	-8
8	13813.975	5			13769.464	-4	16858.592	3
9	13819.332	-3	13726.335	-5	13769.874	-4	16852.606	1
10	13824.761	11	13722.077	0	13770.336	-2	16845.984	-5
11	13830.207	-5	13717.890	-7	13770.864	12	16838.766	6
12	13835.724	-1	13713.801	-2	13771.418	-1	16830.942	1
13	13841.290	3	13709.801	4	13772.040	0	16822.558	-6
14	13846.900	0	13705.884	1	13772.719	2	16813.670	3
15			13702.066	1	13773.454	2	16804.380	80 *
16			13698.344	-0	13774.249	2	16794.830	307 *
17			13694.722	-3	13775.102	3	16785.738	1330 *
18			13691.214	5	13776.014	2		
19			13687.794	-4	13776.973	-13		
20					13778.020	1		
21					13779.112	1		
22					13780.253	-7		
23					13781.459	-7		
24					13782.726	-0		
25					13784.040	4		
26					13785.392	0		

TABLE 3
Rotational Constants (in cm^{-1}) for the Singlet Electronic States of ScH

v	T_v	B_v	$10^3 \times D_v$	$10^7 \times H_v$	$10^9 \times L_v$	q_v	$10^4 \times q_{Dv}$	$10^6 \times q_{Hv}$	$10^8 \times q_{Lv}$
				$G^1\Pi$					
0	20546.9162(38)	6.43103(96)	6.251(48)	-243.2(84)	602.4(50)	1.2337(17)	-195.28(91)	357.2(16)	-273.47(97)
				$F^1\Sigma^-$					
0	19071.6409(24)	4.89702(10)	0.2625(12)	0.465(48)	-0.0457(64)	--	--	--	--
				$D^1\Pi$					
0	16845.6112(23)	4.57582(11)	-0.0348(15)	-3.887(79)	0.323(14)	0.029897(56)	-0.4494(61)	0.0443(16)	--
				$C^1\Sigma^+$					
1	14942.6916(22)	4.60161(34)	1.226(17)	-120.7(29)	10.6(16)	--	--	--	--
0	13574.2537(16)	4.79756(33)	0.512(17)	-3.7(29)	-13.1(16)	--	--	--	--
				$B^1\Pi$					
2	8083.2722(27)	4.63173(14)	0.3098(21)	-0.78(12)	-0.056(24)	0.033881(71)	-0.147(10)	-0.0231(36)	--
1	6767.2388(11)	4.772049(59)	0.30970(76)	-0.410(36)	-0.1358(57)	0.033414(32)	-0.0440(34)	-0.05243(84)	--
0	5404.1857(12)	4.915088(49)	0.29981(44)	0.327(15)	-0.2634(16)	0.033883(43)	-0.1151(54)	0.0224(21)	-0.01266(24)
				$A^1\Delta$					
0	4185.3804(24)	4.665103(84)	0.18514(73)	-0.030(18)	--	--	0.02395(46)	--	--
				$X^1\Sigma^+$					
1	1546.9729(15)	5.238179(89)	0.2674(15)	1.415(96)	-0.417(20)	--	--	--	--
0	0.0	5.363018(20)	0.252817(85)	0.09524(99)	--	--	--	--	--

experimentally. The ScH and ScD bands located at 860.35 nm (11 620 cm^{-1}) and 859.6 nm (11 630 cm^{-1}), respectively, remain unanalyzed because of their complex rotational structure. The appearance of these bands is similar to the $^3\Phi - a^3\Delta$ transition of YH at 11 500 cm^{-1} and the analogous transition of LaH at 6238 cm^{-1}.

1. *The $D^1\Pi - X^1\Sigma^+$ and $D^1\Pi - A^1\Delta$ Transitions of ScH and ScD*

The bands observed with Q heads at 16 846 and 12 643 cm^{-1} for ScH have been assigned as the 0–0 bands of the $D^1\Pi - X^1\Sigma^+$ and $D^1\Pi - A^1\Delta$ transitions, respectively. The $D^1\Pi - X^1\Sigma^+$ band is much weaker in intensity than the $D^1\Pi - A^1\Delta$ band.

As expected, the $D^1\Pi - X^1\Sigma^+$ 0–0 band consists of a single R, a single Q, and a single P branch. The lines in these branches could be followed up to $R(13)$, $Q(15)$, and $P(15)$. The lines have a typical width of 0.05 cm^{-1} independent of J, consistent with negligible hyperfine structure. Perturbations have been observed in both the e and f parity levels of the $D^1\Pi$ state. The e level is perturbed at $J' = 8$ while the f level is perturbed at $J' = 11$. The perturbation in the e-parity level shifts the lines by approximately -0.40 cm^{-1} while the perturbation in the f-parity level shifts the lines by $+0.26$ cm^{-1}. The analysis of this band indicates the presence of large Λ doubling ($q = 0.02990$ cm^{-1}) in the $D^1\Pi$ state.

The $D^1\Pi - A^1\Delta$ band consists of two R, two Q, and two P branches. The doubling in the lines is a reflection of the large Λ doubling in the $D^1\Pi$ state. The $A^1\Delta$ state has nearly negligible Λ doubling but a higher order Λ-doubling parameter q_D is required to obtain a satisfactory fit of the observed lines. The perturbations in the $D^1\Pi$ state observed in the analysis of the $D^1\Pi - X^1\Sigma^+$ transition were confirmed in the $D^1\Pi - A^1\Delta$ transition. A part of the spectrum of the Q branch near the origin is presented in Fig. 2. The perturbation at $Q_{ef}(8)$ can clearly be seen in this figure.

The corresponding $D^1\Pi - X^1\Sigma^+$ and $D^1\Pi - A^1\Delta$ bands of ScD are located at 16 883 and 12 661 cm^{-1}. The f-parity levels of the $^1\Pi$ state are perturbed for $J' \geqslant 15$. The perturbation in the e levels could not be detected in the observed

TABLE 4
Rotational Constants (in cm^{-1}) for the Singlet Electronic States of ScD

v	T_v	B_v	$10^4 \times D_v$	$10^8 \times H_v$	$10^{12} \times L_v$	q_v	$10^5 \times q_{Dv}$	$10^8 \times q_{Hv}$	$10^9 \times q_{Lv}$
				$G^1\Pi$					
0	20556.5124(49)	2.90870(30)	6.576(52)	83.2(25)	--	0.30023(19)	-67.76(54)	49.3(46)	4.36(17)
				$F^1\Sigma^-$					
2	b+13767.8775(16)	2.45959(14)	0.6845(80)	0.47(17)	--	--	--	--	--
1	20131.7467(19)	2.502858(47)	0.6353(30)	-0.200(55)	--	--	--	--	--
0	19089.4490(13)	2.545613(18)	0.66086(44)	0.2430(28)	--	--	--	--	--
				$E^1\Delta$					
1	a+12889.4267(26)	2.47392(14)	0.7234(81)	--	--	--	--	--	--
0	17146.6655(17)	2.519397(37)	0.7058(21)	0.336(36)	--	--	0.1742(14)	--	--
				$D^1\Pi$					
0	16882.7024(28)	2.43298(12)	0.669(17)	29.18(76)	--	0.00839(12)	-0.84(26)	29.3(13)	--
				$C^1\Sigma^+$					
1	14592.5291(23)	2.43221(10)	1.006(13)	-27.72(44)	--	--	--	--	--
0	13602.6808(11)	2.482491(49)	0.7762(49)	-8.82(14)	--	--	--	--	--
				$B^1\Pi$					
2	b	2.43517(15)	0.7766(86)	0.95(17)	--	0.005791(24)	0.186(12)	--	--
1	6418.6526(15)	2.479421(54)	0.8515(60)	8.40(22)	-52.2(18)	0.006453(49)	-1.076(78)	7.97(29)	--
0	5432.3501(10)	2.520158(18)	0.70501(55)	0.4193(61)	-0.695(23)	0.008432(50)	-0.0575(15)	0.01853(98)	--
				$A^1\Delta$					
1	a	2.36849(12)	0.5028(65)	--	--	--	--	--	--
0	4222.3050(19)	2.412930(41)	0.5260(23)	0.122(37)	--	--	--	0.0591(48)	--
				$X^1\Sigma^+$					
2	2208.2518(27)	2.672516(69)	0.6403(35)	--	--	--	--	--	--
1	1116.5052(11)	2.718896(19)	0.66106(52)	--	--	--	--	--	--
0	0.0	2.764728(14)	0.66777(33)	0.1324(20)	--	--	--	--	--

Note: a and b represent the undetermined positions of v=1 and v=2 vibrational levels of the $A^1\Delta$ and $B^1\Pi$ states, respectively.

range of J values. The lines involving the e-parity levels of the $D^1\Pi$ state have been observed only up to $J' = 11$ in the $D^1\Pi - A^1\Delta$ bands and only the Q branch was identified in the $D^1\Pi - X^1\Sigma^+$ 0–0 band.

2. *The $E^1\Delta - A^1\Delta$ and $E^1\Delta - B^1\Pi$ Transitions of ScD*

The ScD bands with 0–0 band origins at 12 924 and 11 714 cm^{-1} have been assigned as the 0–0 bands of the $E^1\Delta - A^1\Delta$ and $E^1\Delta - B^1\Pi$ transitions. Since the ScH bands are, in general, weaker in intensity than the ScD bands, the corresponding ScH bands could not be analyzed in this case.

A part of the P branch of the $E^1\Delta - A^1\Delta$ 0–0 band of ScD is presented in Fig. 3. The lines of this band consist of two R and two P branches. The doubling in the lines of this band results from the relatively large Λ doubling in the $E^1\Delta$ state compared to that in the $A^1\Delta$ state. The 1–1, 2–2, and 3–3 bands are also present to higher wavenumbers. A rotational analysis of the 1–1 and 2–2 bands was also obtained. The $E^1\Delta - B^1\Pi$ transition of ScD is much weaker in intensity than the $E^1\Delta - A^1\Delta$ transition and only the 0–0 band was rotationally analyzed. The R, Q, and P lines of this transition are also doubled because of the presence of Λ doubling in both states. A part of the Q branch near the origin is presented in Fig. 4. The Q_{ef} and Q_{fe} branches are well resolved and move in opposite directions with increasing J because of the large Λ doubling in the $B^1\Pi$ state.

3. *The $F^1\Sigma^- - B^1\Pi$ Transition of ScH and ScD*

The 0–0 band with a single R, a single Q, and a single P branch at 13 668 cm^{-1} of ScH has been assigned as the $F^1\Sigma^- - B^1\Pi$ transition. The lower state combination differences from the R and P branches of this band match very well with the f-parity combination differences of the $B^1\Pi$ state indicating that the excited $^1\Sigma$ state is in fact a $^1\Sigma^-$ state.

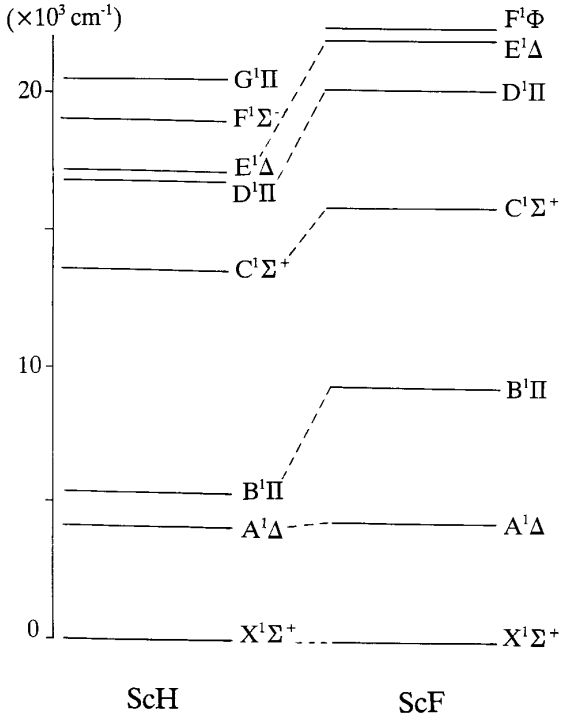

FIG. 6. A correlation energy level diagram for the known singlet electronic states of ScH and ScF.

Anglada *et al.* (*13*) predict a $^1\Sigma^- - B^1\Pi$ transition at 12 500 cm^{-1} consistent with the present observations.

The corresponding ScD $F^1\Sigma^- - B^1\Pi$ 0–0 band is located at 13 657 cm^{-1}. The lines of this band can be followed up to $R(31)$, $P(31)$, and $Q(33)$. Part of the Q branch of the 0–0 band of ScD is provided in Fig. 5 and some low J lines near the head have been marked.

The molecular constants of the different electronic states have been determined using the following customary energy level expressions for $^1\Sigma$ (Eq. [1]) and $^1\Pi$ and $^1\Delta$ (Eq. [2]) states:

$$F_v(J) = T_v + B_vJ(J+1) - D_v[J(J+1)]^2 + H_v[J(J+1)]^3 + L_v[J(J+1)]^4 \quad [1]$$

$$F_v(J) = T_v + B_vJ(J+1) - D_v[J(J+1)]^2 + H_v[J(J+1)]^3 + L_v[J(J+1)]^4 \pm 1/2\{qJ(J+1) + q_D[J(J+1)]^2 + q_H[J(J+1)]^3 + q_L[J(J+1)]^4\}. \quad [2]$$

The observed line positions were weighted on the basis of the signal-to-noise ratio and the extent of blending. The lines involved in perturbations were excluded from the fit, although the corresponding lower state combination differences were included. Because of perturbations in many of the excited states, several higher order effective rotational and Λ-doubling constants were required to obtain a satisfactory fit of the observed line positions. The line positions of the ScH and ScD bands are provided in Tables 1 and 2 and the molecular constants for all of the singlet states of ScH and ScD are provided in Tables 3 and 4.

DISCUSSION

The recent MRD-CI calculations of Anglada *et al.* (*13*) predict the relative energies and transition moments for many electric dipole-allowed transitions with an uncertainty of about ±2000 cm^{-1} for the electronic energies. The positions of the different electronic transitions observed in the present work are in good agreement with the calculations of Anglada *et al.* (*13*) within the error limit of the calculations. For example, the $D^1\Pi - X^1\Sigma^+$ and the $D^1\Pi - A^1\Pi$ transitions have been predicted to be at 18 160 and 13 710 cm^{-1} with transition moments of 1.58 and 1.09 D, respectively, while the observed transitions are located at 16 846 and 12 661 cm^{-1}. The intensity of the observed transitions agrees only moderately well with the calculated transition dipole moments presumably because of additional interactions. The $E^1\Delta - A^1\Delta$ and $E^1\Delta - B^1\Pi$ transitions of ScH are predicted to be at 15 000 and 12 990 cm^{-1} with transition dipole moments of 1.01 and 0.61 D, respectively. These transitions have not been analyzed for ScH, although they are found at 12 925 and 11 715 cm^{-1} for ScD. The next electronic state that we have seen above the $E^1\Delta$ state is the $F^1\Sigma^-$ state, although there should also be a nearby $^1\Sigma^+$ state. The $F^1\Sigma^-$ state has an allowed transition at 13 657 cm^{-1} to the $B^1\Pi$

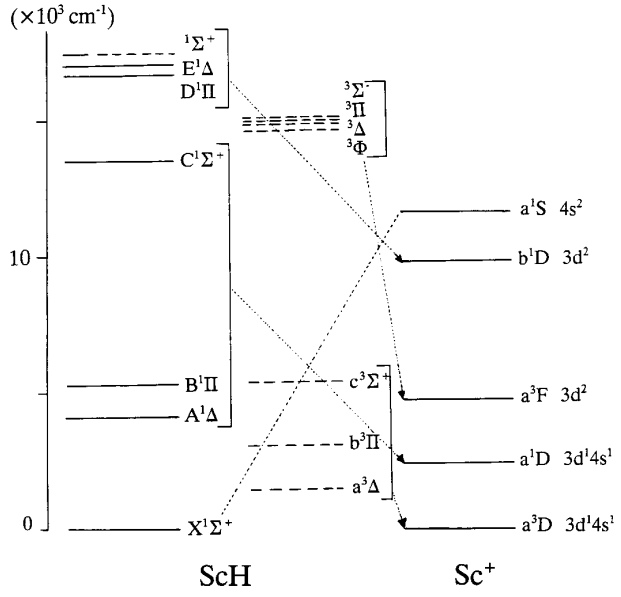

FIG. 7. A correlation energy level diagram of the electronic states of ScH and Sc^+. The energy levels of ScH indicated by dashed lines have been taken from the theoretical calculations of Anglada *et al.* (*13*) and the atomic energy levels are from Moore (*24*).

TABLE 5
Equilibrium Constants (in cm^{-1}) for the New Singlet States of ScD

Const.[a]	$A^1\Delta$	$E^1\Delta$	$F^1\Sigma^-$
$\Delta G(1/2)$	--	--	1042.2977(23)
B_e	2.435150(76)	2.542136(81)	2.567039(97)
α_e	0.04444(13)	0.04548(15)	0.04284(13)
r_e(Å)	1.895011(30)	1.854706(29)	1.845688(35)

[a]The numbers in parentheses are one standard deviation in the last two digits.

state for ScH compared to the calculated value of 12 500 cm^{-1} [1.55 D]. In addition to these new transitions the previously reported transitions $B^1\Pi-X^1\Sigma^+$ (5404 cm^{-1}), $C^1\Sigma^+-X^1\Sigma^+$ (13 574 cm^{-1}), and $G^1\Pi-X^1\Sigma^+$ (20 547 cm^{-1}) have been predicted by Anglada *et al.* (*13*) at 7420 cm^{-1} (0.2 D), 15 160 cm^{-1} (1.42 D), and 23 330 cm^{-1} (0.77 D), respectively.

As has been noticed previously, a strong correspondence exists between the electronic states of transition metal hydrides and the corresponding fluorides. The correspondence between CoH (*17*) and CoF (*18*), and FeH (*19, 20*) and FeF (*21*) has been discussed previously. The ScH and ScF molecules show a similar effect. A comparison of the known singlet electronic states of ScH and ScF is provided in Fig. 6. The data for ScF have been taken from the recent work of Shenyavskaya *et al.* (*22*) and Lebeault-Dorget *et al.* (*23*).

We have also tried to correlate the molecular energy levels of ScH with the energy levels of Sc^+ (*24*). This correspondence was excellent for Fe^+, FeH, and FeF (*21*) as well as for Co^+, CoH, and CoF (*18*) but is not very good in the Sc^+, ScH, and ScF case (Figs. 6 and 7). The main problem is that the ground state $X^1\Sigma^+$ state correlates to the high-lying a^1S Sc^+ state arising from the $4s^2$ Sc^+ configuration. Interestingly, at the Hartree–Fock level of theory, this $^1\Sigma^+$ state of ScH is high-lying with a ground $^3\Delta$ state but with electron correlation the $^1\Sigma^+$ state is strongly stabilized and becomes the ground state (*13*). In fact it was primitive Hartree–Fock calculations on ScH that erroneously suggested that ScH, YH, and LaH might have $^3\Delta$ ground states (*11*).

In the language of ligand field theory, the presence of an F^- or H^- ligand near Sc^+ causes the more polarizable $4s^2$ $X^1\Sigma^+$ state to be strongly stabilized relative to the $4s3d$ $a^3\Delta$ state (*25*). If this ''problem'' is overlooked, then the correlation between the other low-lying states of Sc^+, ScH, and ScF is reasonably good (Figs. 6 and 7).

From the point of view of molecular orbital theory (*13*), the ground $X^1\Sigma^+$ state arises from the $7\sigma^2$ configuration while the $a^3\Delta$ and $A^1\Delta$ states come from the $7\sigma1\delta$ configuration. The 7σ orbital is a bonding $Sc(4s + 4p\sigma) + H(1s)$ orbital and the 1δ orbital is the $Sc(3d\delta)$ orbital. The other states generally follow the common pattern of states and configurations shared by the ScH, YH, LaH, TiO, ZrO, and HfO family of molecules.

The spectroscopic constants for various electronic states of ScH (Table 3) and ScD (Table 4) have been used to calculate equilibrium molecular parameters. The equilibrium constants for the $X^1\Sigma^+$, $B^1\Pi$, and $C^1\Sigma^+$ states of ScH and ScD have been provided in our previous paper (*14*). The equilibrium constants for the $A^1\Delta$, $E^1\Delta$, and $F^1\Sigma^-$ states of ScD are provided in Table 5.

CONCLUSION

The electronic spectra of ScH and ScD have been investigated in the visible and near infrared regions using a Fourier transform spectrometer. In addition to the $B^1\Pi-X^1\Sigma^+$, $C^1\Sigma^+-X^1\Sigma^+$, and $G^1\Pi-X^1\Sigma^+$ transitions of ScH and ScD reported previously (*14*), we have analyzed the new $D^1\Pi-X^1\Sigma^+$, $D^1\Pi-A^1\Pi$, and $F^1\Sigma^--B^1\Pi$ transitions for ScH and the new $D^1\Pi-X^1\Sigma^+$, $D^1\Pi-A^1\Pi$, $E^1\Delta-A^1\Delta$, $E^1\Delta-B^1\Pi$, and $F^1\Sigma^--B^1\Pi$ transitions for ScD. A fit of the data for ScH and for ScD has been obtained and the position of nearly all of the singlet electronic states below 21 000 cm^{-1} is now known. The singlet electronic states of ScH and ScD have been found to correlate well with the observed singlet electronic states of ScF. Our observations are also consistent with the results of the recent high-quality theoretical calculations of Anglada *et al.* (*13*).

ACKNOWLEDGMENTS

We thank J. Wagner and C. Plymate of the National Solar Observatory for assistance in obtaining the spectra. The National Solar Observatory is operated by the Association of Universities for Research in Astronomy, Inc., under contract with the National Science Foundation. The research described here was supported by funding from the NASA laboratory astrophysics program. Support was also provided by the Natural Sciences and

Engineering Research Council of Canada and the Petroleum Research Fund administered by the American Chemical Society.

REFERENCES

1. K. Balasubramanian and J. Z. Wang, *J. Mol. Spectrosc.* **133,** 82–89 (1989).
2. R. S. Ram and P. F. Bernath, *J. Chem. Phys.* **101,** 9283–9288 (1994).
3. R. S. Ram and P. F. Bernath, *J. Mol. Spectrosc.* **171,** 169–188 (1995).
4. K. K. Das and K. Balasubramanian, *Chem. Phys. Lett.* **172,** 372–378 (1990).
5. R. S. Ram and P. F. Bernath, *J. Chem. Phys.* **104,** 6444–6450 (1996).
6. R. E. Smith, *Proc. R. Soc. London A* **332,** 113–127 (1973).
7. A. Bernard, C. Effantin, and R. Bacis, *Can. J. Phys.* **55,** 1654–1656 (1977).
8. C. W. Bauschlicher, Jr. and S. P. Walch, *J. Chem. Phys.* **76,** 4560–4563 (1982).
9. J. Anglada, P. J. Bruna, S. D. Peyerimhoff, and R. J. Buenker, *J. Mol. Struct.* **93,** 299–305 (1983).
10. P. J. Bruna and J. Anglada, *in* ''Quantum Chemistry: The Challenge of Transition metals and Coordination Chemistry'' (A. Veillard, Ed.), p. 67, Reidel, Dordrecht, 1986.
11. P. R. Scott and W. G. Richards, *J. Phys. B* **7,** 1679–1682 (1974).
12. D. P. Chong, S. R. Langhoff, C. W. Bauschlicher, Jr., S. P. Walch, and H. Partridge, *J. Chem. Phys.* **85,** 2850–2860 (1986).
13. J. Anglada, P. J. Bruna, and S. D. Peyerimhoff, *Mol. Phys.* **66,** 541–563 (1989).
14. R. S. Ram and P. F. Bernath, *J. Chem. Phys.* **105,** 2668–2674 (1996).
15. R. S. Ram and F. Bernath, *J. Chem. Phys.* **96,** 6344–6347 (1992).
16. B. A. Palmer and R. Engleman, ''Atlas of the Thorium Spectrum.'' Los Alamos National Laboratory, Los Alamos, 1983.
17. R. S. Ram, P. F. Bernath, and S. P. Davis, *J. Mol. Spectrosc.* **175,** 1–6 (1996).
18. R. S. Ram, P. F. Bernath, and S. P. Davis, *J. Chem. Phys.* **104,** 6949–6955 (1996).
19. S. R. Langhoff and C. W. Bauschlicher, Jr., *J. Mol. Spectrosc.* **141,** 243–257 (1990).
20. J. G. Phillips, S. P. Davis, B. Lindgren, and W. J. Balfour, *Astrophys. J. Suppl.* **65,** 721–778 (1990).
21. R. S. Ram, P. F. Bernath, and S. P. Davis, *J. Mol. Spectrosc.* **179,** 282–298 (1996).
22. E. A. Shenyavskaya, A. J. Ross, T. Topauzkhanian, and G. Wannous, *J. Mol. Spectrosc.* **162,** 327–334 (1994).
23. M.-A. Lebeault-Dorget, C. Effantin, A. Bernard, J. D'Incan, J. Chevaleyre, and E. A. Shenyavskaya, *J. Mol. Spectrosc.* **163,** 276–283 (1994).
24. C. E. Moore, ''Atomic Energy Levels,'' Vol. I. Natl. Bur. of Standards, Washington, DC, 1949.
25. H. Schall, M. Dulick, and R. W. Field, *J. Chem. Phys.* **87,** 2898–2912 (1987).